npj | materials degradation

Article

Published in partnership with CSCP and USTB

https://doi.org/10.1038/s41529-024-00460-y

Effect of hydrogen embrittlement on mechanical characteristics of DLC-coating for hydrogen valves of FCEVs

Dong-Ho Shin [1] & Seong-Jong Kim [2]

Diamond-like carbon (DLC) coating is a surface coating technology with excellent hydrogen permeation resistance and wear resistance. However, it is difficult to completely prevent hydrogen permeation, and when hydrogen penetrates into the coating layer, the DLC coating is adversely affected. Therefore, we investigated the effect of hydrogen embrittlement on the adhesion strength and wear resistance of the DLC coating layer. As the results of the research, the surface roughness of the DLC coating was increased by a maximum of 3.8 times with hydrogen charging, and the delamination ratio of the DLC coating reached about 58%. In addition, the Lc3, which refers to the adhesion strength corresponding to the complete delamination of the DLC coating, was decreased by a maximum of 2.0 N due to hydrogen permeation. In addition, the wear resistance decreased due to hydrogen permeation, and the exposed width of the substrate due to wear increased by more than 4 times. It was also determined that hydrogen blistering or hydrogen-induced cracking occurred at the interface between the DLC coating and the chromium buffer layer due to hydrogen permeation, which decreased the durability of the DLC coating.

Climate change is a growing problem due to global warming and air pollution[1]. In particular, various greenhouse gases, such as carbon dioxide, methane, and nitrogen dioxide, are emitted from automobiles using fossil fuels, which is attracting attention as a factor that accelerates environmental pollution. Thus, researchers are very interested in researching and developing eco-friendly power sources to replace fossil fuels[2,3].

Among the various alternative power sources, hydrogen fuel cells represent an eco-friendly power source due to having a relatively fast response and high efficiency, in addition to emitting only water[4]. Fuel cell electric vehicles (FCEVs) that use hydrogen fuel cells can be manufactured with various systems and parts, such as a hydrogen supply system, hydrogen storage system, hydrogen fuel cells, power trains, etc. In particular, the hydrogen supply system is an essential system that safely supplies and shuts off the hydrogen fuel from the hydrogen tank to the fuel cells[5].

In terms of the components of the hydrogen supply system, the hydrogen valve requires particularly high durability due to being the component that operates most frequently during the operation of FCEVs. In particular, the plunger, which is one of the parts of the hydrogen valve, is made of steel that is worn by friction with the core due to the reciprocating motion. This decreases both the performance and lifespan of the hydrogen valve, and in severe cases, the operation of FCEVs may be impossible due to valve malfunction. Moreover, in an environment in which hydrogen exists, wear increases dramatically due to the defects and cracks formed through hydrogen permeation into the surface of the plunger or core[6]. As a consequence, it is essential to apply a surface coating technology that exhibits both excellent hydrogen permeation resistance and excellent wear resistance.

There are many surface coating technologies with excellent hydrogen permeation resistance and wear resistance[7,8]. Among them, the diamond-like carbon (DLC) coating is known to form a barrier layer with excellent hydrogen permeation resistance and wear resistance due to its inherent structure and characteristics[9,10]. In general, the DLC coating consists of an amorphous carbon structure in which a graphite structure (sp^2) and a diamond structure (sp^3) are mixed, as well as in which the sp^3 ratio is higher, so it is called DLC coating[11]. In particular, the sp^3 structure has a relatively dense structure due to the compressive residual stress. Therefore, it exhibits excellent hydrogen permeation resistance and wear resistance[12,13]. In light of these advantages, researchers have investigated the hydrogen permeation resistance of DLC coatings.

[1]Department of Marine Engineering, Graduate School, Mokpo National Maritime University, 91, Haeyangdaehak-ro, Mokpo-si, Jeollanam-do, Republic of Korea. [2]Division of Marine System Engineering, Mokpo National Maritime University, 91, Haeyangdaehak-ro, Mokpo-si, Jeollanam-do, Republic of Korea. e-mail: ksj@mmu.ac.kr

M. Tamura et al. investigated the hydrogen barrier characteristic of DLC-coated stainless steel and reported that the DLC coating layer decreased hydrogen permeation into the stainless steel about 1000 times[14]. In particular, they found that the hydrogen barrier function was improved when the chromium buffer layer was formed before the DLC coating process. In addition, G.A. Abbas et al. examined the barrier performance of various DLC coatings, finding that the Si-doped hydrogenated amorphous DLC coating was associated with lower internal residual stress, decreased surface defects, and improved barrier performance[15]. However, according to R. Lu et al., the DLC coating has a low diffusion coefficient for hydrogen but does not completely prevent hydrogen permeation[16]. Moreover, T. Michler et al. reported that defects such as cracks and pinholes on the surface of the DLC coating act as pathways through which hydrogen can penetrate into the inside of the coating[17]. According to C. Gu et al., when hydrogen permeates into the coating layer, the adhesion strength of the coating layer is degraded, and ultimately, the coating peels off[18]. Thus, the DLC coating exhibits relatively good resistance to hydrogen permeation, but does not completely prevent hydrogen permeation. In particular, when the DLC coating is damaged due to a decrease in its adhesion strength as a result of hydrogen permeation, its wear resistance decreases sharply due to the associated increase in the surface roughness and destruction of the DLC coating layer. Therefore, it is necessary to investigate the effect of hydrogen embrittlement on the adhesion strength and wear resistance of DLC coatings.

In this research, DLC-coated stainless steel was used to improve the hydrogen permeation resistance, as well as the adhesion strength and wear resistance, which was investigated by means of scratch and reciprocating wear experiments after performing the hydrogen charging experiment on the DLC coating.

Results and discussion

Characteristics of DLC-coated stainless steel

Figure 1 presents the cross-section and surface analysis results of the DLC-coated stainless steel derived by FE-SEM. In this research, the DLC coating was deposited on the surface of the stainless steel by the arc ion plating method, which entails relatively high ionization energy when compared with other physical vapor deposition (PVD) methods and enhances the adhesion strength of both the coating layer and the substrate[19]. Generally, to improve the adhesion strength of the DLC coating, a very thin chromium buffer layer (about 60 nm) is deposited on the stainless steel substrate using a chromium target (purity of 99.8%) in an argon environment, and then the DLC coating layer (about 700 nm) is deposited on the chromium buffer layer[20,21]. In particular, the chromium buffer layer, which represents an interlayer between the DLC coating layer and the substrate, has been found to more effectively prevent hydrogen permeation[14]. As a result of the cross-sectional observations, the chromium buffer layer and DLC coating layer were deposited densely and uniformly, and each interface was clearly observed. In addition, defects such as cracks and pinholes were not found in the coating layer, buffer layer, and interface between the layers. By contrast, through the surface observations, micro-particles and pores of various sizes were observed on the surface of the DLC coating. These micro-particles are formed during the coating process, and they are fragmented after colliding with other micro-particles, forming defects such as pores and pinholes during the deposition process[22]. The micro-pores are formed approximately 2 μm in size, which is sufficiently large for molecular hydrogen (H_2), atomic hydrogen (H), and hydrogen ions (H^+) to permeate and be trapped. In a hydrogen valve operating environment in which high-pressure hydrogen gas exists, hydrogen collides with micro-particles to promote the formation of defects on the coating surface due to damage or delamination. According to Lee et al., mechanical characteristics are significantly reduced by hydrogen permeation in the presence of defects such as pores and cracks on the surface of the metal rather than in the presence of dislocations inside the metal[23]. As a result, micro-particles and micro-defects on the surface of the DLC coating are thought to be factors that accelerate both hydrogen attack and hydrogen embrittlement. Therefore, a critical task is to reduce micro-particles and defects on the DLC coating surface and prevent substrate exposure. These can be achieved in three ways. The first is to completely remove the impurities inside the chamber and on the surface of the substrate. In practice, however, it is very difficult to completely remove impurities. The second method is to increase the thickness of DLC coating. The sizes of defects on DLC coating decrease with increasing coating thickness because of compressive residual stress[24–27]. However, as thickness increases, the residual stress also rises at the same time, possibly reducing the durability of the coating layer and precluding the complete prevention of substrate exposure. The third approach is multilayer coating. When DLC is deposited in multiple layers, the locations of the defects are staggered, which is thought to be more effective in preventing substrate exposure[28].

Morphological analysis

Figure 2 depicts the surface roughness measurement results of the DLC coating after the hydrogen charging experiments. Many researchers have conducted electrochemical hydrogen charging and high-pressure hydrogen gaseous experiments to investigate the hydrogen embrittlement of materials exposed to hydrogen environments[29,30]. In addition, the current density corresponding to the actual environments was investigated by comparing the experimental methods. In most research, however, electrochemical hydrogen charging and high-pressure gaseous experiments presented different characteristics depending on the material[31,32]. In practice, the hydrogen gas pressure of approximately 24 bar reaches the hydrogen valve, which is the target of this study. However, it is difficult to determine the current density corresponding to 24 bar in evaluating the durability of the valve. This research also is an accelerated experiment to investigate damage to DLC coatings in the actual operating environments of hydrogen valves. After hydrogen charging experiment, the seven points of damaged specimen were measured using a 3D confocal laser microscope, and after excluding the maximum and minimum values, a value approximated to the average and a 3D image were used. The measurements revealed the surface roughness of the DLC coating without hydrogen charging to be about 0.269 μm. However, under the experimental conditions of the applied current density of 50 mA cm^{-2}, 100 mA cm^{-2}, and 150 mA cm^{-2}, the surface

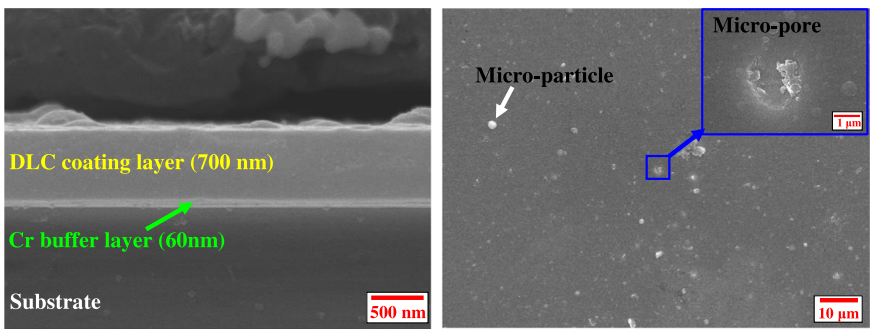

Fig. 1 | Microstructure of DLC coated specimen. Cross-sectional images and surface morphologies of DLC coated 316 L stainless steel.

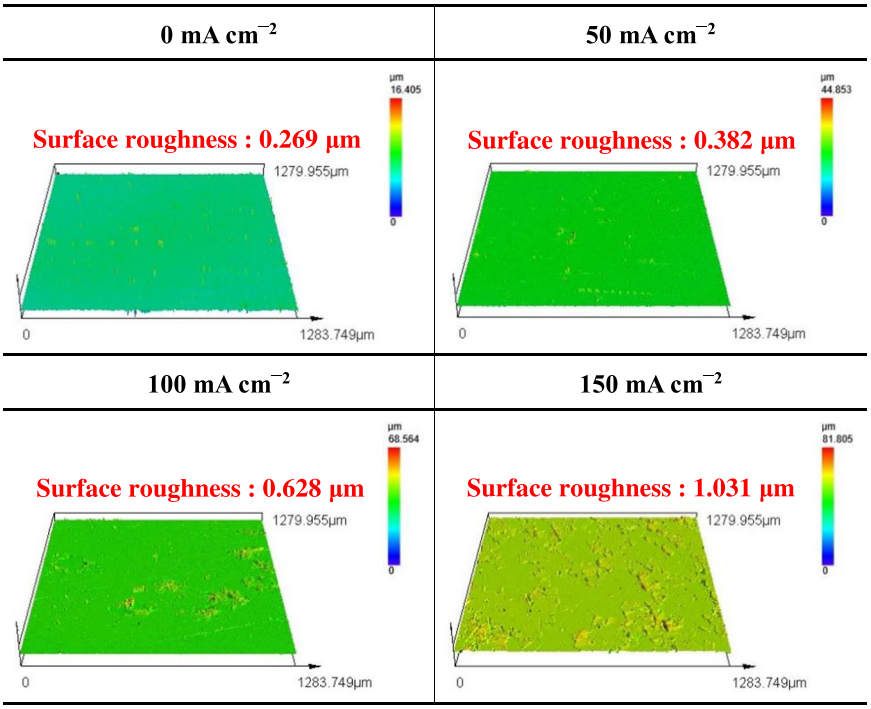

Fig. 2 | The variation of surface roughness by hydrogen charging. 3D images and surface roughness analysis of damaged surface after hydrogen charging (0, 50, 100, 150 mA cm^{-2}) for DLC coated 316 L stainless steel.

roughness was found to be about 0.382 μm, 0.628 μm, and 1.031 μm, respectively. In addition, the surface roughness of the DLC coating increased by up to 3.8 times as the applied current density used for the hydrogen charging increased. This is considered to be due to damage and delamination of the DLC coating by hydrogen permeation.

Figure 3 presents the degree of damage to the DLC coating as the applied current density increases, using a 3D confocal laser microscope. In the case of an applied current density of 50 mA cm^{-2}, a blister shape due to the hydrogen blistering was observed on the surface of the DLC coating. In addition, micro-pinholes were observed in the center of the blister, and the chromium buffer layer was exposed. In particular, the depth of the exposed part was about 0.71 μm (red color), which was fairly similar to the thickness of the DLC coating. At an applied current density of 100 mA cm^{-2}, a crater shape was observed, and the exposed area of the chrome buffer layer was larger due to the cracking and local delamination of the coating in the center of the crater. Moreover, damage to both the buffer layer and the substrate due to hydrogen permeation appeared in the chromium buffer layer. The crater shape was formed by the advance of cracks at the interface between the buffer layer and the substrate due to the hydrogen blistering and formation of the blister on the coating. When the elastic energy exceeds the fracture toughness of the DLC coating layer, the coating layer is damaged and fractured[33]. With regard to an applied current density of 150 mA cm^{-2}, the damage and delamination in relation to the DLC coating were more clearly observed, and the exposed area of the chromium buffer layer was increased dramatically. In particular, in terms of the non-peeled off coating layer, a protrusion shape was observed at the edge of the exposed buffer layer. This protrusion shape is considered to stem from the surface of the DLC coating being swollen due to hydrogen blistering or hydrogen-induced cracking caused by the permeation and molecularization of hydrogen atoms into the interface between the DLC coating layer and chromium buffer layer. During this process, a micro-space is formed at the interface between the DLC coating layer and chromium buffer layer, which causes a local decrease in the adhesion strength of the DLC coating. Thus, the blister and the protrusion shape formed on the surface of the DLC coating increase the surface roughness of the coating, accelerate the damage and delamination caused to the DLC coating by external forces, and act as factors that dramatically decrease the durability of the coating. On these bases, it is very important to prevent the initial permeation and damage to DLC coatings by hydrogen. In particular, DLC coating is expected to remain durable if hydrogen permeation-induced blisters and protrusions are prevented from forming on its surface.

Figure 4 depicts the results of the FE-SEM observations and EDS analysis of the damaged and peeled off surface of the DLC coating following the hydrogen charging experiments. In the case of the DLC coating surface without hydrogen charging, only micro-particles and micro-defects were observed, and the carbon components were mostly measured over the entire surface. However, damage and delamination were observed in relation to the DLC coating after the hydrogen charging experiments, and the Fe and Cr components were clearly observed due to the exposure of the chromium buffer layer as the applied current density increased. In addition, significant surface damage to the exposed chromium buffer layer was observed under the experimental conditions of applied current density of 100 mA cm^{-2} and higher. When stainless steel is exposed due to the delamination of the DLC coating, hydrogen penetrates into its surface, causing cracks and damage to the surface of the substrate due to hydrogen embrittlement[34,35]. In particular, under the experimental condition of an applied current density of 100 mA cm^{-2}, multiple relatively small surface damages were found on the substrate. However, in the case of an applied current density of 150 mA cm^{-2}, relatively large surface damages were observed. The damage is thought to have grown into large damage through the increasing and combining of the multiple small pieces of surface damage as the applied current density increased. In this way, as the size of the surface damage increases, the stress energy is concentrated, degrading the mechanical characteristics and durability with even a small amount of external stress[36,37].

Figure 5 reveals the delamination ratio of the DLC coating layer after the hydrogen charging, using Image J software. As a result of the calculations, the delamination ratio of the DLC coating with the applied current density of 50 mA cm^{-2}, 100 mA cm^{-2}, and 150 mA cm^{-2} was 1.94%, 13.08%, and 58.28%, respectively. At an applied current density of 150 mA cm^{-2}, the delamination ratio was the largest when compared with the other applied current density. In general, the DLC coating layer exhibits excellent hydrogen permeation resistance. However, the delamination of the DLC coating is accelerated because the hydrogen permeation resistance is rapidly reduced from the start point of damage and delamination with regard to the

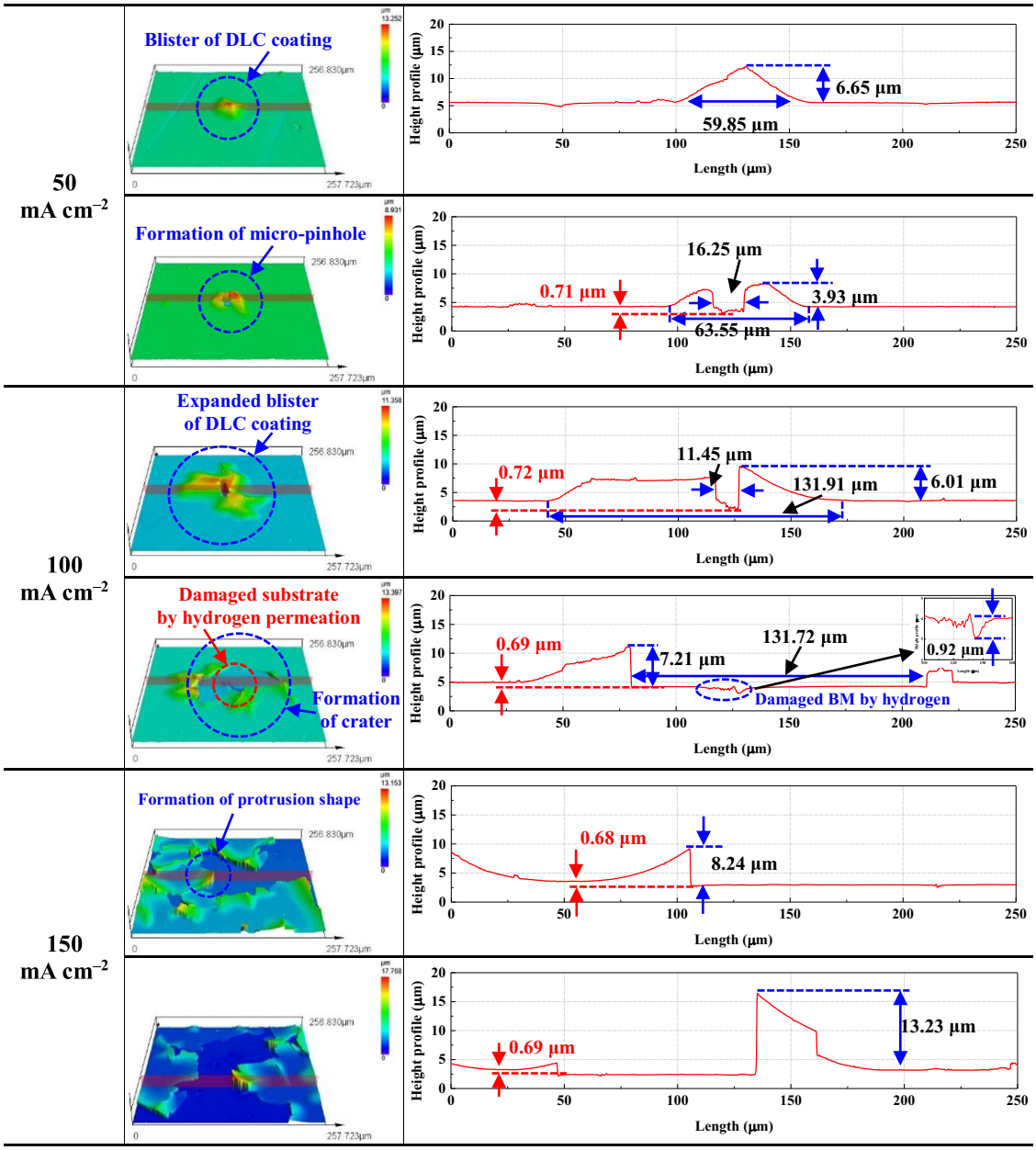

Fig. 3 | The variation of surface damage degree by hydrogen charging. 3D images and profile analysis of delaminated DLC coating layer after hydrogen charging (0, 50, 100, 150 mA cm^{-2}) for DLC coated 316 L stainless steel.

coating layer. Delaminated DLC coatings can migrate into a fuel cell and cause electrolyte degradation. In severe cases, they can block hydrogen gas piping and valves, making it impossible to supply hydrogen gas to the fuel cell and thereby hindering the operation of the cell. These results may be caused more significantly by hydrogen embrittlement or friction/wear of the material itself, not just the coating. Nevertheless, DLC coatings were chosen for this research because of their relatively high resistance to hydrogen embrittlement and wear. In addition, the DLC coating is considered to have excellent performance as a thin film and will not block the passage of hydrogen gas. Correspondingly, the initial damage and delamination of DLC coatings must be avoided to prevent hydrogen embrittlement.

To summarize the findings depicted in Figs. 3–5, the interfacial space between the DLC coating layer and chromium buffer layer is formed and expanded by hydrogen permeation, which is considered to be a factor that accelerates the damage and delamination of the coating due to the decrease in the adhesion strength and the accumulation of elastic energy.

Adhesion strength

Figure 6 presents the results of the scratch experiment performed to measure the adhesion strength of the DLC coating following the hydrogen charging. In the scratch experiment, the scratch tip was brought into contact with the coating surface under a specific load, and then the coating surface was moved while the load was maintained or increased. This represents a practical method that can be used to evaluate the adhesion strength of a coating by analyzing the acquired data (e.g., tip penetration depth, acoustic emission signal) and the shape of cracks formed on the coating surface by the scratches using an optical microscope[38]. In particular, the adhesion strength is closely related to the durability of the coating[39–41]. Therefore, in this research, the adhesion strength of the DLC coating according to the hydrogen charging was measured and evaluated quantitatively. To accomplish this, three critical loads measured through the scratch experiments were defined[42,43]. The first critical load (Lc1) was the initiation of the initial cracking of the coating, the second critical load

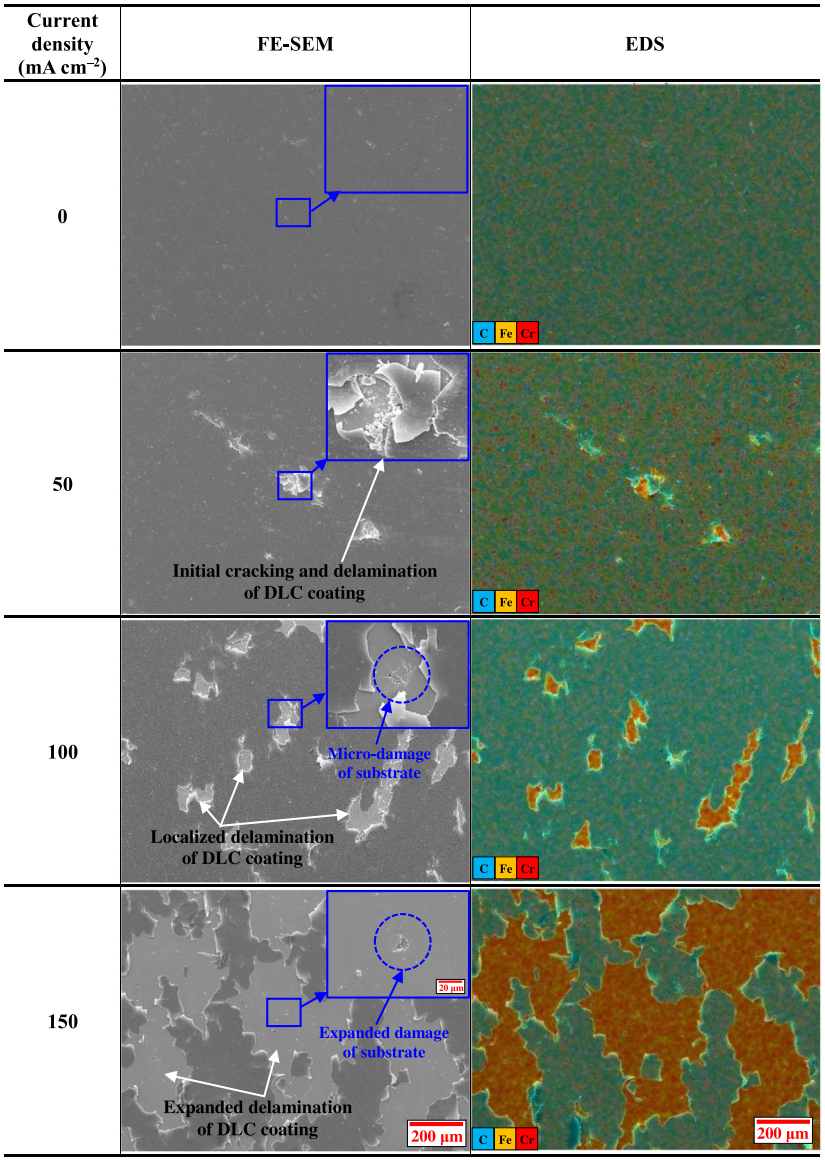

Fig. 4 | The variation of surface morphologies by hydrogen charging. FE-SEM images and EDS analysis of damaged DLC coating layer after hydrogen charging (0, 50, 100, 150 mA cm^{-2}) for DLC coated 316 L stainless steel.

(Lc2) was the chipping caused by the coating cracking and partially delaminating, and the third critical load (Lc3) was the complete destruction of the coating caused by the continuous and complete delamination (spalling). As shown in Fig. 6a, in the case of the DLC coating without hydrogen charging, the first acoustic emission signal peak and the initial cracking of the coating were observed at an applied load of about 2.1 N (Lc1). Afterward, the peak of the acoustic emission signal with the damage to the DLC coating was continuously measured as the applied load increased, and the initial and partial delamination of the coating was observed at about 6.3 N (Lc2). Finally, spalling occurred along the scratch path due to the continuous and complete delamination of the coating at about 7.6 N (Lc3), indicating the complete destruction of the coating. However, all the critical loads (Lc1, Lc2, and Lc3) decreased as the applied current density increased. When comparing the applied current density of 0 mA cm^{-2} and 150 mA cm^{-2}, Lc1 presented a decrease of about 0.5 N; however, Lc2 and Lc3 decreased by 1.4 and 2.0 N, respectively. In particular, Lc2 indicated the largest decrease of about 0.9 N in the range of applied current density from 100 to 150 mA cm^{-2}, although Lc3 decreased the most (to about 1 N) in the range of applied current density from 0 to 50 mA cm^{-2}. Based on these results, it can be seen that the hydrogen embrittlement had a great effect on the adhesion strength of the DLC coating.

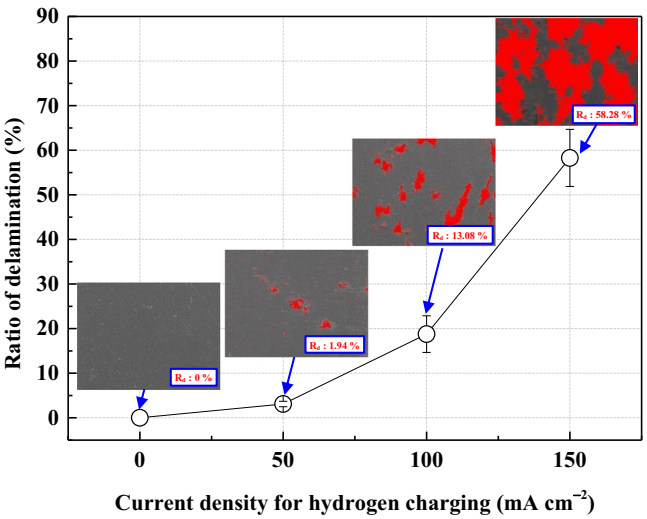

Fig. 5 | The variation of delamination ratio(R_d). Delamination ratio and optical images of damaged DLC coating layer after hydrogen charging (0, 50, 100, 150 mA cm^{-2}) for DLC coated 316 L stainless steel.

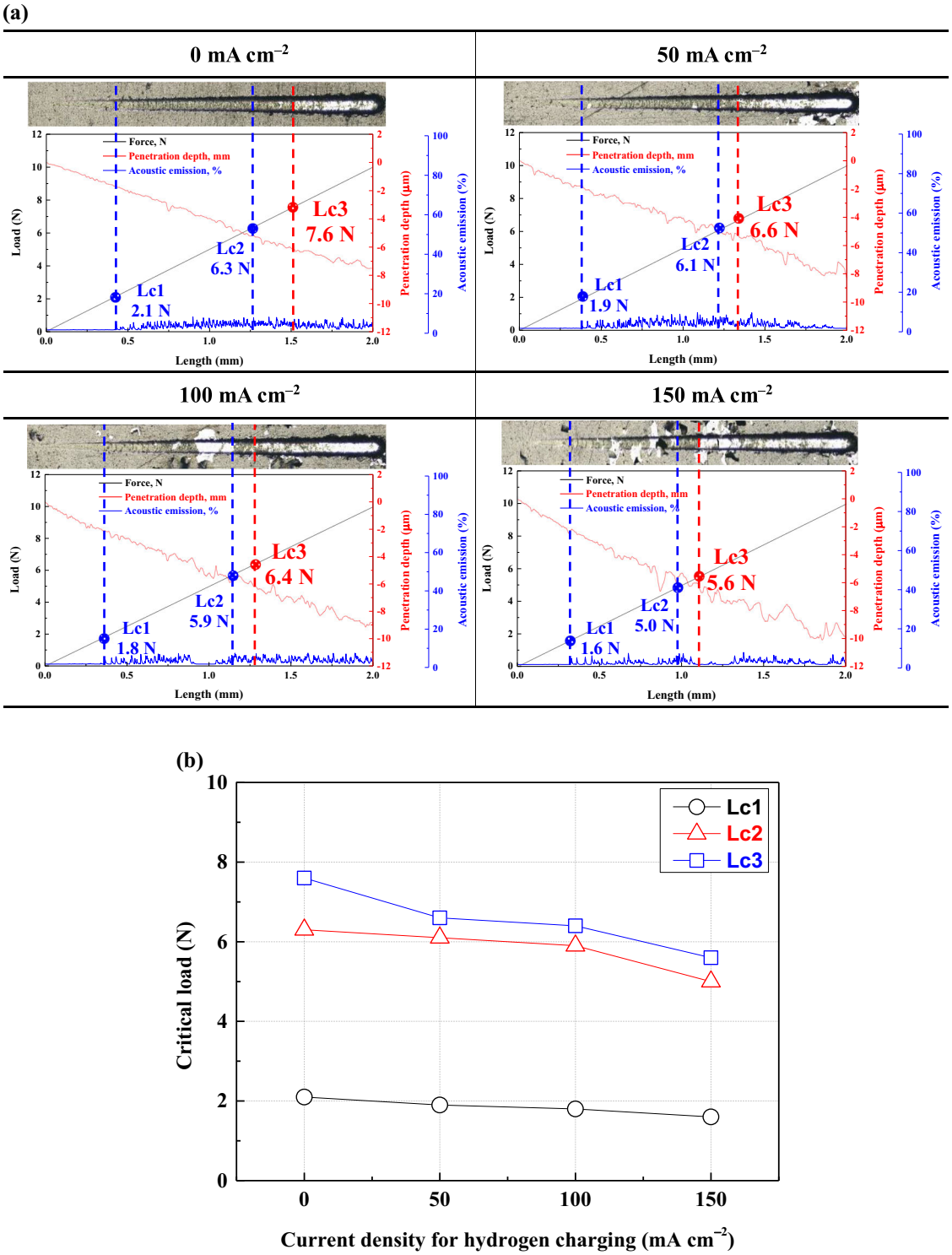

Fig. 6 | Adhesion characteristics after hydrogen charging (0, 50, 100, 150 mA cm^{-2}) of DLC-coated 316 L stainless steel. a Scratch experiment results. **b** Critical load (Lc1: Initial cracking, Lc2: Chipping and partially delamination, Lc3: Complete destruction).

Friction and wear behavior

Figure 7 depicts the friction coefficients determined by the reciprocating friction experiment. Due to the nature of the experiment, the friction coefficients demonstrate positive and negative values depending on the direction. However, the frictional forces of the material can be evaluated and compared with each other based on the width of the friction coefficients. As illustrated in Fig. 7a, the DLC coating without hydrogen charging reached a friction coefficient of 0.6 μ as the substrate was exposed at about 488 m of sliding distance. However, with the increasing applied current density of 50 mA cm^{-2}, 100 mA cm^{-2}, and 150 mA cm^{-2}, the sliding distance decreased to 430 m, 339 m, and 295 m, respectively. The largest decrease of about 91 m was observed under the experimental conditions of applied current density of 50–100 mA cm^{-2}. It is thought that the coating was peeled off in a shorter period of time due to the decrease in the durability of the coating caused by the hydrogen embrittlement. To analyze the change in the friction coefficient with the sliding distance in more detail, the graph of Fig. 7a was enlarged and exhibited as in Fig. 7b. In addition, the width of the friction coefficient was divided into three parts to obtain the initial friction

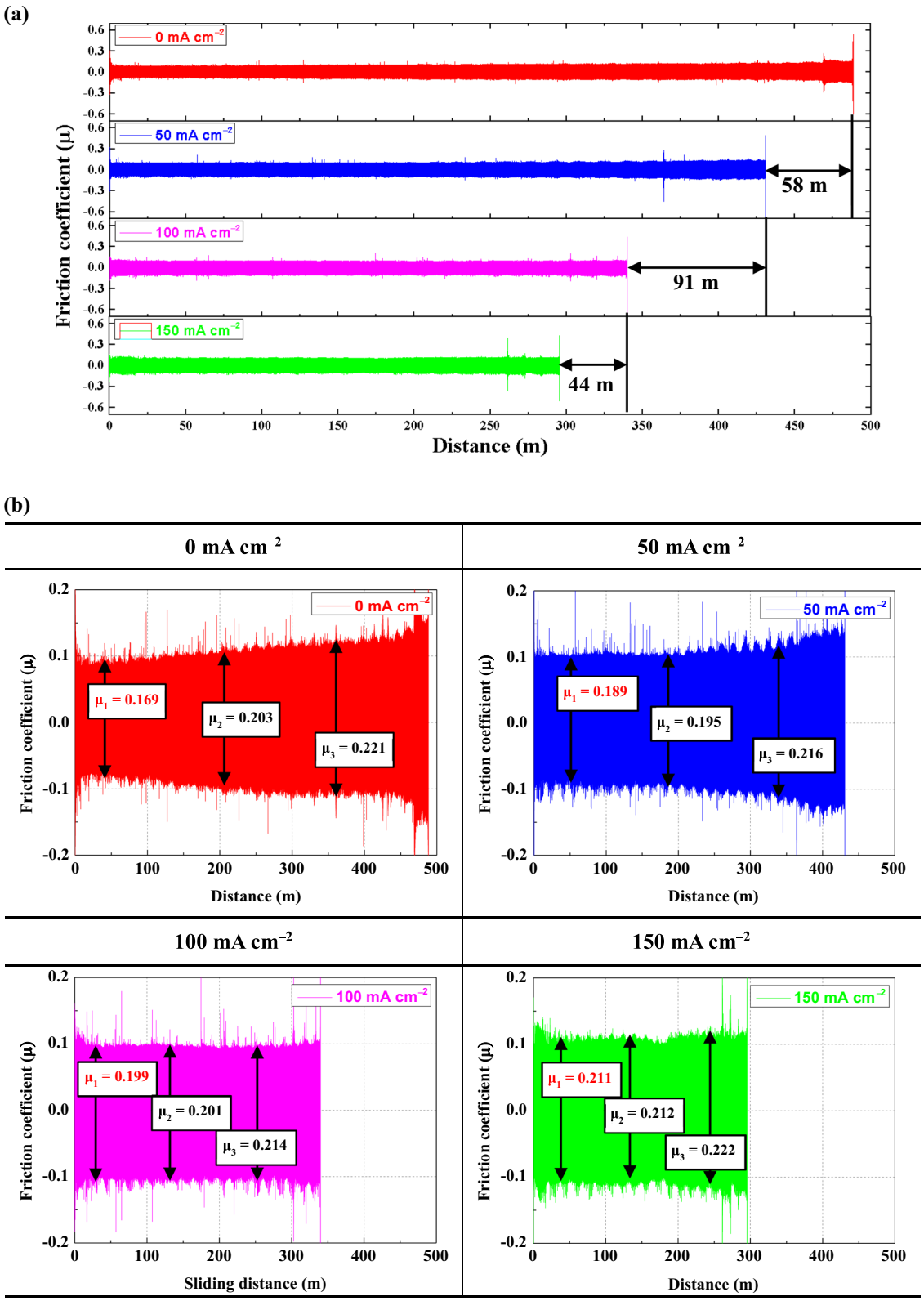

Fig. 7 | Friction coefficient after hydrogen charging (0, 50, 100, 150 mA cm^{-2}) of DLC coated 316 L stainless steel. a Friction coefficient for comparison of DLC coating delamination distance. **b** Friction coefficient according to distance.

coefficient width (μ_1), the intermediate friction coefficient width (μ_2), and final friction coefficient width (μ_3), which were compared. At 0 mA cm^{-2}, the μ_1 was measured as about 0.169 μ, which was relatively low. In general, DLC coatings exhibit high hardness, excellent thermal stability, smooth surface, and self-lubricating (solid lubricating) characteristics, which result in excellent wear resistance[44–48]. In particular, DLC coatings have a very low friction coefficient, which minimizes the generation of the frictional heat that causes wear damage and provides excellent wear resistance because the adhesive force between the contact surfaces is relatively low[49,50]. In terms of the friction experiment results, the friction coefficient of the DLC coating

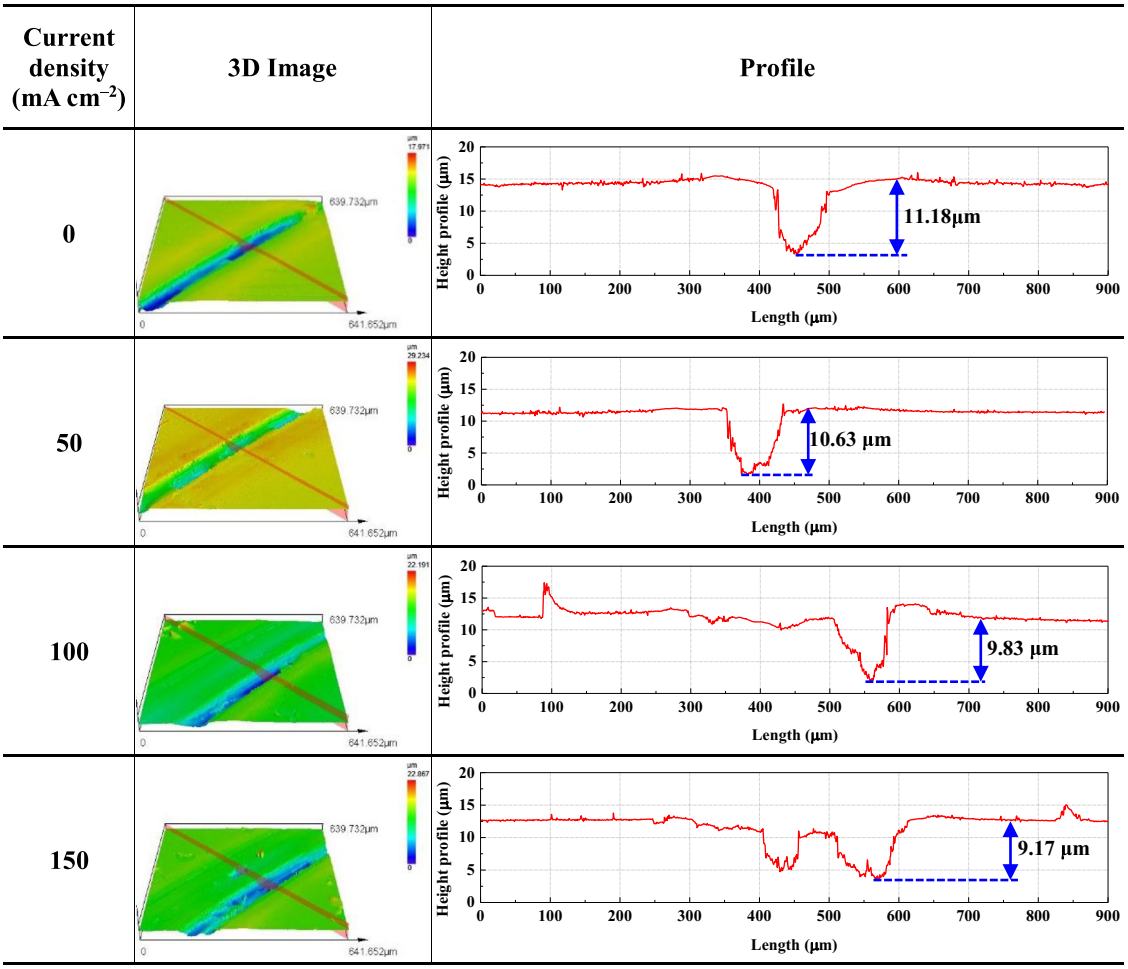

Fig. 8 | The variation of wear track by hydrogen charging. 3D images and profile analysis after friction experiment with hydrogen charging (0, 50, 100, 150 mA cm^{-2}) of DLC-coated 316 L stainless steel.

without hydrogen charging was about 0.085 μ (half of the μ_1 of 0.169 μ), indicating a low friction coefficient and excellent wear resistance. However, as the sliding distance increased, the width of the friction coefficient also increased. This increase in the width of the friction coefficient with the increasing sliding distance indicated a similar trend under all the experimental conditions. However, for the applied current density of 100 mA cm^{-2} and 150 mA cm^{-2}, the width of friction coefficient presented almost similar values for μ_1, μ_2, and μ_3. In addition, in the case of μ_1, the friction coefficient presented a relatively large increase according to the increase in the applied current density. However, μ_3 presented almost similar values under all the experimental conditions. In particular, when comparing the applied current density of 0 mA cm^{-2} and 50 mA cm^{-2} with hydrogen charging, μ_1 increased by about 0.02 μ. In this way, while the effect of hydrogen permeation in the coating is relatively small, it can have a large effect on the wear resistance of the coating. Moreover, when the DLC coating is partially damaged or peeled off, the wear resistance function of the coating is lost and the durability of both the coating layer and the substrate is rapidly reduced.

Figures 8 and 9 present 3D images of the wear tracks and the measurement results of the depth and width of the wear damage observed using a 3D confocal laser microscope. In general, wear products (wear debris, wear particles, etc.) are generated by the work hardening and phase transformation of the contact surface that occurs during friction experiments, which accumulate at the edge of the wear track to form a ridge[51]. This shape is one of the main factors that accelerate wear damage, as plasticized parts are peeled off by frictional wear[52]. However, in the case of the DLC coating used in this research, a ridge shape caused by the wear products was not observed. This is thought to be because the surface is not plasticized due to the wear characteristics of the DLC coating, and as a result, no wear products are formed. In addition, the frictional heat is relatively low, so the tendency toward abrasive wear was more dominant than that toward adhesive wear[53,54]. As demonstrated in Fig. 9a, the wear depth of the DLC coating without hydrogen charging presented a wear depth of about 11.18 μm, while the increasing applied current density of 50 mA cm^{-2}, 100 mA cm^{-2}, and 150 mA cm^{-2} resulted in wear depths of 10.63 μm, 9.83 μm, and 9.17 μm, respectively. As the result, the wear depth presented a decreasing trend as the applied current density increased. In this research, to improve the adhesion strength of the DLC coating on the stainless steel, a chromium buffer layer of 60 nm in thickness was first deposited on the stainless steel and then the DLC coating was deposited, meaning that the adhesion strength of the coating was relatively excellent. In general, the coating layer is worn by shear force during friction experiments[55]. In particular, when the DLC coating thickness is reduced by wear, the compressive residual stress and adhesion strength of the coating are both reduced[56,57]. At the same time, when a shear force stronger than the compressive residual stress and adhesion strength of the coating is applied, the interface destruction between the coating and substrate is accelerated, resulting in damage and delamination of the coating[58]. According to A. A. Voevodin et al., when a contact load is applied to the coating layer with the wear resistance, the strongest shear force is distributed at the interface between the coating and substrate[59]. When the coating thickness is relatively thin, the shear force and frictional heat act more strongly on the substrate to plastically deform it, ultimately causing the adhesion failure of the coating[60–63]. Therefore, when a strong shear force is applied while a certain adhesion strength is retained due to the wear of the coating, the coating is peeled off and the buffer layer or substrate is

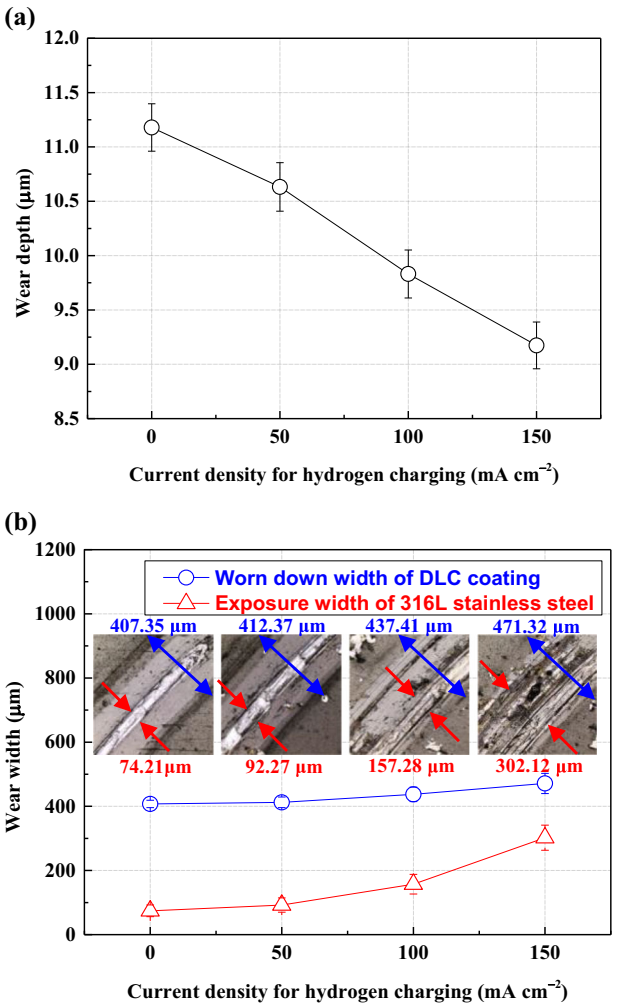

Fig. 9 | The variation of wear degree by hydrogen charging. Wear depth, width, and surface roughness after friction experiment with hydrogen charging (0, 50, 100, 150 mA cm^{-2}) of DLC-coated 316 L stainless steel. **a** Wear depth. **b** Wear width.

plasticized and eventually detached, resulting in adhesive wear[64]. This tendency is reflected in the results of this research. However, as described in Fig. 9b, the wear width exhibited a tendency to increase with an increasing applied current density. In particular, the exposed width of the 316 L stainless steel presented a relatively large increase with an increasing applied current density. The exposed width of the substrate at the applied current density of 0 mA cm^{-2} and 150 mA cm^{-2} was 74.21 μm and 302.12 μm, respectively, which indicated a more than 4 times increase. This is thought to be because the adhesion strength of DLC coating layer and the chromium buffer layer is locally lowered by hydrogen permeation. As a result, the exposed width of the substrate is increased due to partial or complete delamination of the coating by wear damage in a relatively wide range. These results are considered to be due to the following causes. First, the adhesion strength of the DLC coating layer and the chromium buffer layer is locally lowered by hydrogen permeation. Afterward, the coating is partially or completely peeled off by friction to increase the exposed width of the substrate.

Figure 10 depicts the results of the FE-SEM observations and EDS analysis of the damaged surface by wear of the DLC coating. In terms of the worn surface of the DLC coating without the hydrogen charging, abrasive wear was evident in the area where the DLC coating layer remained (i.e., the outer part of the wear track). By contrast, the central part where the substrate was exposed presented damage due to adhesive wear. As mentioned above, the DLC coating has a low friction coefficient, high thermal stability, smooth surface finish, and self-lubricating characteristics that prevent adhesion at the interface between the two materials. In other words, as the DLC coating exhibits excellent adhesion resistance, abrasive wear is considered to be dominant[65]. Conversely, the stainless steel has a relatively high friction coefficient and low thermal stability, meaning that adhesion between the two contact materials is easy, which results in adhesive wear due to the shear force[66,67]. However, the surface observation results after friction experiment in this research present adhesive wear due to the adhesion strength of the DLC coating and the substrate. In general, DLC coatings are subject to abrasive wear due to the specific shear force. However, when the thickness of the coating is thinner than the critical value, it cannot tolerate the applied shear force. As a consequence, it is thought that the part of the substrate bonded to the coating layer is peeled off. Thus, the DLC coating exhibits resistance to shear force for even a very thin film of 0.7 μm, and it also exhibits excellent wear resistance. However, when the thickness is reduced as a result of wear to the coating layer, it is considered that the resistance to shear force is lost and the DLC coating exhibits characteristics such as adhesive wear. In the case of the DLC coating with hydrogen charging, the exposed area of the substrate increased. With regard to the applied current density of 100 mA cm^{-2} and 150 mA cm^{-2} when compared with 50 mA cm^{-2}, multiple instances of micro local delamination were observed. In addition, in the case of an applied current density of 50 mA cm^{-2}, wear products such as wear debris were not observed on the surface of the DLC coating. However, plastically deformed parts appeared in the exposed substrate due to the friction between the substrate and the alumina balls, and wear debris of various sizes were observed. The plastic deformation of the substrate and the formation of wear debris were more clearly observed at the applied current density of 100 mA cm^{-2} and 150 mA cm^{-2}. In the case of an applied current density of 100 mA cm^{-2}, cracks in the plastically deformed part first occurred in the exposed substrate, and in severe cases, these cracks were converted into wear debris. These wear debris are formed by the plastic deformation of the metal and the cracks of surface. In addition, the wear debris increases the surface roughness and acts as a factor that lowers wear resistance. However, the DLC coating did not form wear products. In addition, it is thought that excellent wear resistance can be continuously maintained by the remaining DLC coating layer even if the adhesion strength of the coating is reduced and local delamination occurs due to hydrogen charging.

Delamination mechanism of DLC coating layer

Figure 11 illustrates the delamination mechanism of the DLC coating associated with hydrogen charging. Initially, there are micro-cracks and micro-pores on the surface of the DLC coating (1st step). Simultaneously, hydrogen atoms in the hydrogen environment penetrate and diffuse into the interface between the DLC coating layer and chromium buffer layer through the micro-cracks or micro-pores (2nd step). Thereafter, the diffused hydrogen atoms are molecularized to cause the hydrogen blistering. Therefore, the size of the interface region is expanded by vertical stress and a micro-space is formed, thereby decreasing the adhesion strength between the DLC coating layer and the chromium buffer layer (3rd step). During this third step, the degradation of the DLC coating layer is initiated. In addition, the micro-cracks and the blister shapes appear on the surface of the DLC coating by the buckling of the coating layer. Hence, when more hydrogen molecules are generated at the interface between the DLC coating layer and chromium buffer layer, stronger vertical stress acts on the upper surface of the DLC coating layer to cause the growth of the blister on the surface of the coating. In addition, interfacial cracking between the coating layer and buffer layer is promoted. Furthermore, the adhesion strength is almost lost (4th step). If this process has continued, elastic energy exceeding the fracture toughness is accumulated in the DLC coating, and the cracking of the coating layer progresses further. In severe cases, micro-pinholes are formed due to the destruction of the coating layer, and the chromium buffer layer is exposed (5th step). Moreover, as the adhesion strength decreases and is lost in the horizontal direction of the formed pinholes, a crater shape appears due to the local delamination of the DLC coating, and finally, the coating layer completely peels off (6th step).

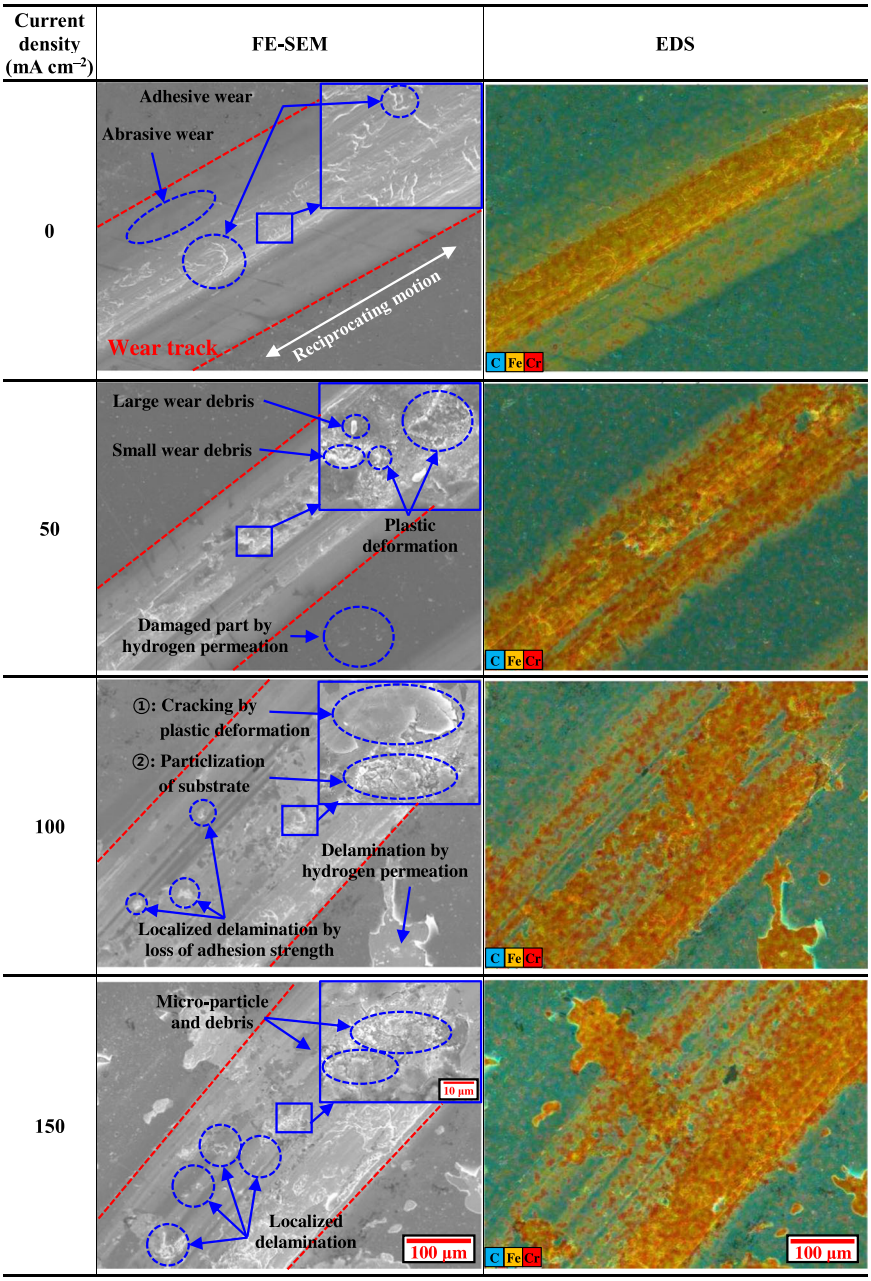

Fig. 10 | Microstructure analysis of wear track by hydrogen charging. FE-SEM images and EDS analysis of worn down surface after friction experiment with hydrogen charging (0, 50, 100, 150 mA cm^{-2}) of DLC coated 316 L stainless steel.

Considerations for application of DLC coating to prevent hydrogen embrittlement

This research examined the resistance of hydrogen embrittlement resistance and wear of DLC coatings to improve the durability of hydrogen valves as components of hydrogen vehicles. In future work, we intend to address the following issues: The first is hydrogen embrittlement on a substrate during glow discharge in a mixed environment of argon and hydrogen gas during DLC coating process. Many researchers have argued that surface coating technology is required in a hydrogen gas-free environment due to the problem of hydrogen embrittlement during glow discharge[68,69]. However, some studies have found no hydrogen embrittlement characteristics in substrates exposed to a mixed environment of hydrogen gas[70,71]. The second issue is the change in the characteristics of DLC coatings due to hydrogen embrittlement. DLC coatings have a combined diamond (sp^3) and graphite (sp^2) structure, and they exhibit different binding energies depending on the fractions of sp^3 and sp^2 in the coatings[72]. In particular, under abundant sp^3, DLC coating has a dense structure and effectively prevents the migration of substances[73,74]. Correspondingly, the binding energies and characteristics of DLC coatings are expected to change because of hydrogen embrittlement. It is therefore necessary to investigate the effects of hydrogen on the crystallographic structure of DLC coating. The third issue for future exploration is that the exposure area of a specimen differs from that of an actual component. In this research, it was necessary to consider the specimen affected by hydrogen and the exposure area of an actual hydrogen valve. However, the error ratio determined by differences in specimen sizes was expected to be small because the experiment was performed under current density. The fourth issue to be addressed in future work is how to effectively prevent hydrogen embrittlement and damage in DLC coatings. As shown in this research, DLC coatings exhibit excellent resistance against hydrogen permeation. However, H_2, H, and H^+ can permeate through surface defects to the interface between the DLC coating layer and the buffer layer or substrate. This problem can be solved by increasing the thickness of DLC coating or performing multilayer deposition. The challenge is that increasing the thickness of DLC coating diminishes the durability of the coating layer

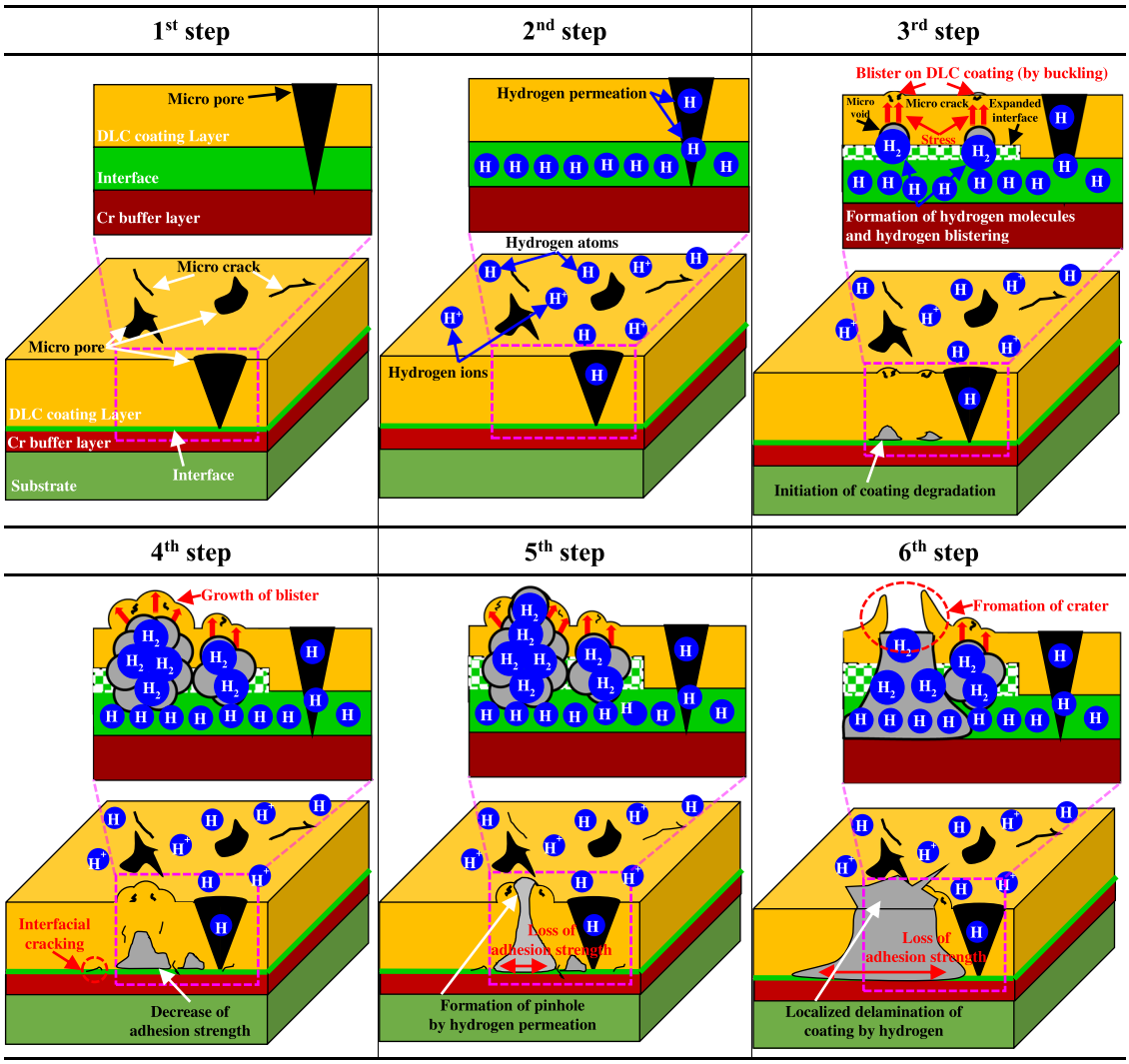

Fig. 11 | Delamination mechanism of DLC coating layer with hydrogen charging of DLC coated 316 L stainless steel. The delamination process of DLC coating layer is divided into six steps, designated as 1st, 2nd, 3rd, 4th, 5th and 6th.

Table 1 | Chemical composition of 316L stainless steel

Ni	Cr	Mo	C	Si	Mn	P	S	Cu	N	Fe
10.19	16.7	2.03	0.023	0.60	1.05	0.034	0.0028	0.282	0.012	Bal.

because of increased residual stress. This phenomenon can produce internal cracks, which can increase the permeation ratio of hydrogen gas[75]. In addition, hydrogenated DLC coatings suffer from various shortcomings, such as poor adhesion to a substrate, limited thickness, the desorption of hydrogen over time, and temperature changes[76–78]. Nevertheless, the multilayer deposition of DLC coatings can increase thickness while simultaneously distributing residual stresses to each layer[79,80]. Surface defects can also be staggered layer by layer to minimize substrate exposure[81]. Therefore, multilayer deposition is considered the optimal coating method, as it presents the strongest resistance against hydrogen embrittlement.

Previous research has found significantly better hydrogen embrittlement resistance by DLC coatings than CrN coatings[82]. In particular, DLC coatings on hydrogen valves that reciprocate for more than approximately twice per second exhibit a significantly lower friction coefficient and are recommended for hydrogen valve applications due to their excellent wear resistance. However, future research on buffer layer materials (deposition force, hydrogen permeation resistance, etc.) is needed depending on type of substrate.

As a result, the DLC coating prevented hydrogen permeation into the substrate and exhibited relatively excellent wear resistance, indicating it to be a surface coating technology that is suitable for use in parts where frictional wear occurs while hydrogen exists. However, the DLC coating could not completely prevent hydrogen permeation, and when hydrogen penetrated into the interface between the coating layer and buffer layer or substrate, the durability of the DLC coating was reduced due to hydrogen molecularization.

We recommend the DLC coating technology for plunger, which is the component of hydrogen valve. This is due to the excellent hydrogen embrittlement resistance and wear resistance of DLC coatings. In particular, DLC coatings exhibit improved performance when surface defects are controlled, when buffer layer materials are used, and when the application environment is considered during deposition. Further research should be directed toward the application of DLC coatings under various conditions.

Methods

Preparation of specimen and DLC coating

The specimen used in this research was 316 L stainless steel and the chemical composition of the stainless steel is depicted in Table 1. To perform the DLC coating process, the specimen was cut to a size of 20 mm × 20 mm and its surface was polished using 4000 grit SiC abrasive paper and 0.3 μm alumina suspension. The polished specimen was then cleaned with ultrasonic waves using acetone and distilled water before being dried in a vacuum dryer for

Table 2 | Condition of DLC coating process by arc ion plating

Parameter	Heating	Glow discharge	Metal etching	Metal coating (Cr)	Carbon etching	Carbon coating
Temp. (°C)	350				130	95
Press. (torr)	~3×10^{-5}	~2.5×10^{-2}	~7×10^{-4}	~2.5×10^{-3}	~2×10^{-4}	~6×10^{-4}
Bias (V)	–	400–500	550	60	750	10
Gas flow (Sccm)	–	Ar:H_2 = 66:34	Ar 25	Ar 100	Ar 4	Ar 5
Time	60	40	1.6	2	2	15

24 h. Subsequently, an amorphous DLC coating was deposited on the stainless steel surface using the arc ion plating method. Chamber pressure and temperature were maintained at 3×10^{-5} Torr and 350 °C, respectively, for 60 min to remove the residual gas and moisture inside the chamber. Argon and hydrogen gas were then injected into the chamber at a ratio of 66:34, and the substrate was glow-discharged for 40 min by applying a bias of 400 to 500 V. The plasma generated in this process ionizes argon and hydrogen gas, thereby removing impurities from the substrate surface and activating it. In this case, hydrogen ions can penetrate the surface of the substrate and give rise to the risk of hydrogen embrittlement. However, according to J. Cwiek, no difference in elongation is found in tensile tests performed with and without hydrogen gas during glow discharge[70]. Furthermore, in the current research, the substrate was exposed to hydrogen for 40 min at a flow rate of 34 sccm, which is a negligible value that is not expected to cause hydrogen embrittlement. After surface cleaning through glow discharge, a chromium buffer layer was deposited onto the surface to improve the adhesion strength of the DLC coating layer. Deposition of the buffer layer was performed in an environment injected with argon at 100 sccm (temperature: 350 °C, pressure: 2.5×10^{-3} Torr) for 2 min. Amorphous DLC coating was then deposited onto the specimen surface via carbon etching and carbon coating. Carbon etching during glow discharge is a preliminary step in improving the deposition performance of DLC coatings. The detailed parameters of the process are shown in Table 2.

Hydrogen charging experiment

To investigate the hydrogen permeation resistance of the DLC-coated stainless steel, hydrogen was artificially charged for 12 h at applied current density of 50 mA cm^{-2}, 100 mA cm^{-2}, and 150 mA cm^{-2} in 2 N H_2SO_4 + 1 g L^{-1} $Na_2HAsO_4 \cdot 7H_2O$ solution using a power supply. Direct current was applied to the DLC-coated specimen (working electrode) as the cathode and the platinum electrode (counter electrode) as the anode. Details are shown in the schematic in Fig. 12. After the hydrogen charging, the surface of the specimen was observed and the surface roughness (Sa) was measured using a three-dimensional (3D) confocal laser microscope (OLS-5000, OLYMPUS, Tokyo, Japan). In addition, the effect of the hydrogen embrittlement on the DLC coating layer was analyzed by means of field emission scanning electron microscopy (FE-SEM, JSM-7500F, JEOL, Tokyo, Japan) and energy-dispersive X-ray spectroscopy (EDS, AZTec Energy, Oxford Instruments, Abingdon, UK) analyses. Moreover, the delamination ratio of the DLC coating was measured using Image J software.

Scratch experiment

To measure the adhesion strength of the DLC coating before and after the hydrogen charging, a micro scratch tester (MCT3, Anton Paar, Garz, Austria) equipped with an optical microscope, an acoustic emission detection system, a tangential friction force sensor, and a penetration depth measurement sensor were used. For the scratch experiment, a Rockwell C diamond indenter with an angle of 120° and a diameter of 100 μm was used. The scratch distance was 2 mm, the load increased linearly from 0.02 N to 10 N, and the scratch rate and load rate were set at 0.5 mm min^{-1} and 2.5 N min^{-1}, respectively. In addition, to ensure reproducibility, the scratch experiment was repeated 14 times under the same conditions. The scratch data were approximated to the average and the results of the optical microscope observations were analyzed.

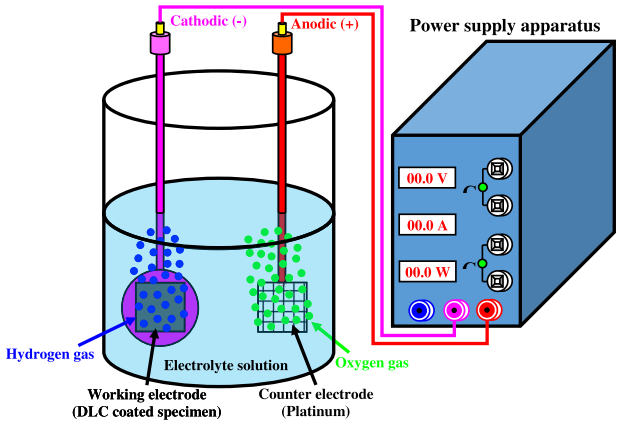

Fig. 12 | Schematic diagram of the hydrogen charging experiment with power supply apparatus in acid solution. These are the illustration of the cathodic hydrogen charging setup and power supply apparatus that applies direct current.

Friction experiment

A friction experiment was conducted to evaluate the frictional wear characteristics of the DLC-coated stainless steel following the hydrogen charging. A tribometer (TRB3, Anton Paar, Graz, Austria) was used for the friction experiment, and a ball-on-disk method was adopted. In addition, to simulate the operating environment of the hydrogen valve, the friction coefficient and sliding distance were measured after the reciprocating wear experiment. The ball used in the experiment was an alumina ball with a diameter of 6 mm and a Vickers hardness of 1650 HV. In terms of the experimental conditions, the rotation radius, reciprocating angle, sliding speed, and applied load of the disk were set as 6 mm, 30°, 3 cm s^{-1}, and 25 N, respectively, while the air temperature and humidity were maintained at 25 °C and 30%, respectively. In addition, to evaluate the durability of the DLC coating layer according to the hydrogen charging, the friction experiment was set to stop when the friction coefficient reached 0.6 μ, and the associations between the sliding distance and the hydrogen charging time were compared. After the experiment, the wear depth, width, and surface roughness of the wear track were measured using a 3D confocal laser microscope to evaluate the wear damage. Furthermore, the worn surface was observed and the chemical composition was analyzed by means of FE-SEM and EDS.

Data availability

All data generated or analyzed during this study are included in this published article, and any additional data that support the findings of this study are available from the corresponding author upon reasonable request.

Received: 25 December 2023; Accepted: 10 April 2024;
Published online: 04 May 2024

References

1. Sekoai, P. T. & Yoro, K. O. Biofuel development initiatives in Sub-Saharan Africa: opportunities and challenges. *Climate* **4**, 33 (2016).
2. Luo, Y. et al. Development and application of fuel cells in the automobile industry. *J. Energy Storage* **42**, 103124 (2021).
3. Olabi, A. G., Wilberforce, T. & Abdelkareem, M. A. Fuel cell application in the automotive industry and future perspective. *Energy* **214**, 118955 (2021).
4. Pei, P. & Chen, H. Main factors affecting the lifetime of Proton Exchange Membrane fuel cells in vehicle applications: a review. *Appl. Energy* **125**, 60–75 (2014).
5. Hwang, H. K., Shin, D. H. & Kim, S. J. Hydrogen embrittlement characteristics by slow strain rate test of aluminum alloy for hydrogen valve of hydrogen fuel cell vehicle. *Corros. Sci. Technol.* **21**, 503–513 (2022).
6. Seo, D. I. & Lee, J. B. Comparison of hydrogen embrittlement resistance between 2205 duplex stainless steels and type 316L austenitic stainless steels under the cathodic applied potential. *Corros. Sci. Technol.* **15**, 237–244 (2016).
7. Rönnebro, E. C. E., Oelrich, R. L. & Gates, R. O. Recent advances and prospects in design of hydrogen permeation barrier materials for energy applications—a review. *Molecules* **27**, 6528 (2022).
8. Laadel, N. E., El Mansori, M., Kang, N., Marlin, S. & Boussant-Roux, Y. Permeation barriers for hydrogen embrittlement prevention in metals—a review on mechanisms, materials suitability and efficiency. *Int. J. Hydrog. Energy* **47**, 32707–32731 (2022).
9. Hatta, A., Kaneko, S. & Hassan, M. K. Hydrogen permeation through diamond-like carbon thin films coated on PET sheet. *Plasma Process. Polym.* **4**, 241–244 (2007).
10. Lin, Y., Zhou, Z. & Li, K. Y. Improved wear resistance at high contact stresses of hydrogen-free diamond-like carbon coatings by carbon/carbon multilayer architecture. *Appl. Surf. Sci.* **477**, 137–146 (2019).
11. Kim, S. H. & Jang, J. C. Investigation of structural change of DLC coating during frictional wear by Raman spectroscopy. *J. Korean Inst. Surf. Eng.* **52**, 16–22 (2019).
12. Park, M. S., Kim, D. Y., Shin, C. S. & Kim, W. R. Improved adhesion of DLC films by using a nitriding layer on AISI H13 substrate. *J. Korean Inst. Surf. Eng.* **54**, 307–314 (2021).
13. Liechtenstein, V. K., Ivkova, T. M., Spitsyn, A. V. & Olshanski, E. D. A study of very thin DLC foils as a gas barrier. *Nucl. Instrum. Methods Phys. Res. Sect. A Accel. Spectrometers Detect. Assoc. Equip.* **590**, 171–175 (2008).
14. Tamura, M. & Kumagai, T. Hydrogen permeability of diamondlike amorphous carbons. *J. Vac. Sci. Technol. A Vac. Surf. Film.* **35**, 04D101 (2017).
15. Abbas, G. A., McLaughlin, J. A. & Harkin-Jones, E. A study of ta-C, a-C:H and Si-a:C:H thin films on polymer substrates as a gas barrier. *Diam. Relat. Mater.* **13**, 1342–1345 (2004).
16. Lu, R. et al. Effect of diamond-like carbon coating on preventing the ingress of hydrogen into bearing steel. *Tribol. Trans.* **64**, 157–166 (2021).
17. Michler, T. & Naumann, J. Coatings to reduce hydrogen environment embrittlement of 304 austenitic stainless steel. *Surf. Coat. Technol.* **203**, 1819–1828 (2009).
18. Gu, C., Hu, J. & Zhong, X. The coating delamination mitigation of epoxy coatings by inhibiting the hydrogen evolution reaction. *Prog. Org. Coat.* **147**, 105774 (2020).
19. Shi, C. M., Wang, T. G., Pei, Z. L., Gong, J. & Sun, C. Effects of the thickness ratio of CrN vs Cr_2O_3 layer on the properties of double-layered CrN/Cr_2O_3 coatings deposited by arc ion plating. *J. Mater. Sci. Technol.* **30**, 473–479 (2014).
20. Ahmad, I. et al. Substrate effects on the microstructure of hydrogenated amorphous carbon films. *Curr. Appl. Phys.* **9**, 937–942 (2009).
21. Song, J. S. & Nam, T. W. The effects of imterlayer on the DLC coating. *Corros. Sci. Technol.* **10**, 65–70 (2011).
22. Boxman, R. L. & Goldsmith, S. Macroparticle contamination in cathodic arc coatings: generation, transport and control. *Surf. Coat. Technol.* **52**, 39–50 (1992).
23. Guan, X. et al. Microstructures and properties of Zr/CrN multilayer coatings fabricated by multi-arc ion plating. *Tribol. Int.* **106**, 78–87 (2017).
24. Shin, D. H. & Kim, S. J. Electrochemical characteristics and damage behaviour of DLC-coated 316L stainless steel for metallic bipolar plates of PEMFCs. *Trans. Imf.* **101**, 308–319 (2023).
25. Gunnars, J. & Alahelisten, A. Thermal stresses in diamond coatings and their influence on coating wear and failure. *Surf. Coat. Technol.* **80**, 303–312 (1996).
26. Pauleau, Y. Residual stresses in DLC films and adhesion to various substrates. In:Donnet, C., Erdemir, A. (eds) Tribology of Diamond-Like Carbon Films. p. 102–136 (Springer, 2008).
27. Yi, P., Zhang, D., Peng, L. & Lai, X. Impact of film thickness on defects and the graphitization of nanothin carbon coatings used for metallic bipolar plates in proton exchange membrane fuel cells. *ACS Appl. Mater. Interfaces* **10**, 34561–34572 (2018).
28. Dalibon, E. L., Moreira, R. D., Guitar, M. A., Trava-Airoldi, V. J. & Brühl, S. P. Influence of the substrate pre-treatment on the mechanical and corrosion response of multilayer DLC coatings. *Diam. Relat. Mater.* **118**, 108507 (2021).
29. Arniella, V., Zafra, A., Álvarez, G., Belzunce, J. & Rodríguez, C. Comparative study of embrittlement of quenched and tempered steels in hydrogen environments. *Int. J. Hydrog. Energy* **47**, 17056–17068 (2022).
30. Okonkwo, P. C. et al. A focused review of the hydrogen storage tank embrittlement mechanism process. *Int. J. Hydrog. Energy* **48**, 12935–12948 (2023).
31. Djukic, M. B., Bakic, G. M., Zeravcic, V. S. & Sedmak, A. The synergistic action and interplay of hydrogen embrittlement mechanisms in steels and iron: Localized plasticity and decohesion. *Eng. Fract. Mech.* **216**, 106528 (2019).
32. Koren, E. et al. Experimental comparison of gaseous and electrochemical hydrogen charging in X65 pipeline steel using the permeation technique. *Corros. Sci.* **215**, 111025 (2023).
33. Falub, C. V. et al. In vitro studies of the adhesion of diamond-like carbon thin films on CoCrMo biomedical implant alloy. *Acta Mater.* **59**, 4678–4689 (2011).
34. Elhoud, A. M., Renton, N. C. & Deans, W. F. Hydrogen embrittlement of super duplex stainless steel in acid solution. *Int. J. Hydrog. Energy* **35**, 6455–6464 (2010).
35. Murakami, Y., Kanezaki, T. & Mine, Y. Hydrogen effect against hydrogen embrittlement. *Metall. Mater. Trans. A Phys. Metall. Mater. Sci.* **41**, 2548–2562 (2010).
36. Wang, S., Liang, W., Duan, L., Li, G. & Cui, J. Effects of loading rates on mechanical property and failure behavior of single-lap adhesive joints with carbon fiber reinforced plastics and aluminum alloys. *Int. J. Adv. Manuf. Technol.* **106**, 2569–2581 (2020).
37. Li, B., Shen, Y. & Hu, W. Casting defects induced fatigue damage in aircraft frames of ZL205A aluminum alloy—a failure analysis. *Mater. Des.* **32**, 2570–2582 (2011).
38. Ollendorf, H. & Schneider, D. A comparative study of adhesion test methods for hard coatings. *Surf. Coat. Technol.* **113**, 86–102 (1999).
39. Łępicka, M., Grądzka-Dahlke, M., Pieniak, D., Pasierbiewicz, K. & Niewczas, A. Effect of mechanical properties of substrate and coating on wear performance of TiN- or DLC-coated 316LVM stainless steel. *Wear* **382–383**, 62–70 (2017).

40. Shin, D. H. & Kim, S. J. Effect of hydrogen charging on the mechanical characteristics and coating layer of CrN-coated aluminum alloy for light-weight FCEVs. *Jpn J. Appl. Phys.* **62**, 1–10 (2023).
41. Zaidi, H., Djamai, A., Chin, K. J. & Mathia, T. Characterisation of DLC coating adherence by scratch testing. *Tribol. Int.* **39**, 124–128 (2006).
42. Waseem, B. et al. *Optimization and Characterization of Adhesion Properties of DLC Coatings on Different Substrates*. *Materials Today: Proceedings* 2 (Elsevier Ltd., 2015).
43. Jacobs, R. et al. A certified reference material for the scratch test. *Surf. Coat. Technol.* **174–175**, 1008–1013 (2003).
44. Tyagi, A. et al. A critical review of diamond like carbon coating for wear resistance applications. *Int. J. Refract. Met. Hard Mater.* **78**, 107–122 (2019).
45. Erdemir, A. & Martin, J. M. Superior wear resistance of diamond and DLC coatings. *Curr. Opin. Solid State Mater. Sci.* **22**, 243–254 (2018).
46. Wang, L., Wan, S., Wang, S. C., Wood, R. J. K. & Xue, Q. J. Gradient DLC-based nanocomposite coatings as a solution to improve tribological performance of aluminum alloy. *Tribol. Lett.* **38**, 155–160 (2010).
47. Vanhulsel, A. et al. DLC solid lubricant coatings on ball bearings for space applications. *Tribol. Int.* **40**, 1186–1194 (2007).
48. Scharf, T. W. & Prasad, S. V. Solid lubricants: a review. *J. Mater. Sci.* **48**, 511–531 (2013).
49. Fontaine, J., Donnet, C. & Erdemir, A. Fundamentals of the tribology of DLC coatings. *Tribol. Diamond-Like Carbon Film. Fundam. Appl*. 139–154 (2008).
50. Fukui, H., Okida, J., Omori, N., Moriguchi, H. & Tsuda, K. Cutting performance of DLC coated tools in dry machining aluminum alloys. *Surf. Coat. Technol.* **187**, 70–76 (2004).
51. Rao, R. N. & Das, S. Effect of matrix alloy and influence of SiC particle on the sliding wear characteristics of aluminium alloy composites. *Mater. Des.* **31**, 1200–1207 (2010).
52. Mekicha, M. A. et al. Study of wear particles formation at single asperity contact: an experimental and numerical approach. *Wear* **470–471**, 203644 (2021).
53. Harris, S. J., Weiner, A. M. & Meng, W. J. Tribology of metal-containing diamond-like carbon coatings. *Wear* **211**, 208–217 (1997).
54. Zhou, Z. F., Li, K. Y., Bello, I., Lee, C. S. & Lee, S. T. Study of tribological performance of ECR-CVD diamond-like carbon coatings on steel substrates Part 2. The analysis of wear mechanism. *Wear* **258**, 1589–1599 (2005).
55. Kato, K. Wear in relation to friction—a review. *Wear* **241**, 151–157 (2000).
56. Xiao, Y., Shi, W., Han, Z., Luo, J. & Xu, L. Residual stress and its effect on failure in a DLC coating on a steel substrate with rough surfaces. *Diam. Relat. Mater.* **66**, 23–35 (2016).
57. Sheeja, D., Tay, B. K., Leong, K. W. & Lee, C. H. Effect of film thickness on the stress and adhesion of diamond-like carbon coatings. *Diam. Relat. Mater.* **11**, 1643–1647 (2002).
58. Escudeiro, A., Wimmer, M. A., Polcar, T. & Cavaleiro, A. Tribological behavior of uncoated and DLC-coated CoCr and Ti-alloys in contact with UHMWPE and PEEK counterbodies. *Tribol. Int.* **89**, 97–104 (2015).
59. Voevodin, A. A., Iarve, E. V., Ragland, W., Zabinski, J. S. & Donaldson, S. Stress analyses and in-situ fracture observation of wear protective multilayer coatings in contact loading. *Surf. Coat. Technol.* **148**, 38–45 (2001).
60. Bernoulli, D. et al. Improved contact damage resistance of hydrogenated diamond-like carbon (DLC) with a ductile α-Ta interlayer. *Diam. Relat. Mater.* **58**, 78–83 (2015).
61. Bernoulli, D. et al. Contact damage of hard and brittle thin films on ductile metallic substrates: an analysis of diamond-like carbon on titanium substrates. *J. Mater. Sci.* **50**, 2779–2787 (2015).
62. Bernoulli, D. et al. Cohesive and adhesive failure of hard and brittle films on ductile metallic substrates: A film thickness size effect analysis of the model system hydrogenated diamond-like carbon (a-C:H) on Ti substrates. *Acta Mater.* **83**, 29–36 (2015).
63. Okonkwo, P. C., Kelly, G., Rolfe, B. F. & Pereira, M. P. The effect of sliding speed on the wear of steel-tool steel pairs. *Tribol. Int.* **97**, 218–227 (2016).
64. Zhou, Y. et al. Hardness anomaly, plastic deformation work and fretting wear properties of polycrystalline TiN/CrN multilayers. *Wear* **236**, 159–164 (1999).
65. Sui, X., Liu, J., Zhang, S., Yang, J. & Hao, J. Microstructure, mechanical and tribological characterization of CrN/DLC/Cr-DLC multilayer coating with improved adhesive wear resistance. *Appl. Surf. Sci.* **439**, 24–32 (2018).
66. Gaard, A., Hallbäck, N., Krakhmalev, P. & Bergström, J. Temperature effects on adhesive wear in dry sliding contacts. *Wear* **268**, 968–975 (2010).
67. Wei, M. X., Wang, S. Q., Wang, L. & Cui, X. H. Wear and friction characteristics of a selected stainless steel. *Tribol. Trans.* **54**, 840–848 (2011).
68. Mashovets, N. S., Pastukh, I. M. & Voloshko, S. M. Aspects of the practical application of titanium alloys after low temperature nitriding glow discharge in hydrogen-free-gas media. *Appl. Surf. Sci.* **392**, 356–361 (2017).
69. Konno, T. et al. Characterization of carburized layer on low-alloy steel fabricated by hydrogen-free carburizing process using carbon ions. *Diam. Relat. Mater.* **135**, 109816 (2023).
70. Cwiek, J. Hydrogen degradation of high-strength steels. *J. Achiev. Mater. Manuf.* **37**, 193–212 (2009).
71. Shin, D. H. & Kim, S. J. Effects of hard anodizing and plasma ion-nitriding on Al alloy for hydrogen embrittlement protection. *Corros. Sci. Technol.* **22**, 221–231 (2023).
72. Mabuchi, Y., Higuchi, T. & Weihnacht, V. Effect of sp^2/sp^3 bonding ratio and nitrogen content on friction properties of hydrogen-free DLC coatings. *Tribol. Int.* **62**, 130–140 (2013).
73. Park, H. et al. The influence of hydrogen concentration in amorphous carbon films on mechanical properties and fluorine penetration: A density functional theory and: ab initio molecular dynamics study. *RSC Adv.* **10**, 6822–6830 (2020).
74. Liu, L., Lu, F., Tian, J., Xia, S. & Diao, Y. Electronic and optical properties of amorphous carbon with different sp^3/sp^2 hybridization ratio. *Appl. Phys. A Mater. Sci. Process.* **125**, 1–10 (2019).
75. Dorner, A. et al. Diamond-like carbon-coated Ti6A14V: influence of the coating thickness on the structure and the abrasive wear resistance. *Wear* **249**, 489–497 (2001).
76. Vasquez-Borucki, S., Jacob, W. & Achete, C. A. Amorphous hydrogenated carbon films as barrier for gas permeation through polymer films. *Diam. Relat. Mater.* **9**, 1971–1978 (2000).
77. Capote, G., Bonetti, L. F., Santos, L. V., Trava-Airoldi, V. J. & Corat, E. J. Adherent amorphous hydrogenated carbon films on metals deposited by plasma enhanced chemical vapor deposition. *Thin Solid Films* **516**, 4011–4017 (2008).
78. Akasaka, H. et al. Thermal decomposition and structural variation by heating on hydrogenated amorphous carbon films. *Diam. Relat. Mater.* **101**, 107609 (2020).
79. Lara, L. C., Costa, H. & De Mello, J. D. B. Influence of layer thickness on sliding wear of multifunctional tribological coatings. *Ind. Lubr. Tribol.* **67**, 460–467 (2015).
80. Djabella, H. & Arnell, R. D. Finite element comparative study of elastic stresses in single, double layer and multilayered coated systems. *Thin Solid Films* **235**, 156–162 (1993).
81. Mingge, W., Congda, L., Tao, H., Guohai, C. & Donghui, W. Chromium interlayer amorphous carbon film for 304 stainless steel bipolar plate of proton exchange membrane fuel cell. *Surf. Coat. Technol.* **307**, 374–381 (2016).
82. Shin, D. H. & Kim, S. J. Effect of hydrogen charging on the mechanical characteristics and coating layer of CrN-coated aluminum alloy for light-weight FCEVs. *Jpn J. Appl. Phys.* **62**, SN1004 (2023).

Acknowledgements
This work was supported by the Advanced Reliability Engineering for Automotive Electronics based on Bigdata Technique Infra (P0021563: Development of Lightweight Hydrogen Valve Module), funded by the Ministry of Trade, Industry & Energy (MOTIE), Republic of Korea.

Author contributions
Dong-Ho Shin: Conceptualization, methodology, investigation, data curation, validation, writing—original draft. Seong-Jong Kim: Conceptualization, formal analysis, funding acquisition, writing—reviewing & editing. All authors reviewed and approved the manuscript.

Competing interests
The authors declare no competing interests.

Additional information
Correspondence and requests for materials should be addressed to Seong-Jong Kim.